



ELSEVIER

## SVX', the new CDF silicon vertex detector

P. Azzi<sup>b</sup>, N. Bacchetta<sup>b,f</sup>, B.A. Barnett<sup>d</sup>, M. Bailey<sup>h</sup>, F. Bedeschi<sup>c</sup>, D. Bisello<sup>b</sup>, J.D. Cammerata<sup>d</sup>, W.C. Carithers<sup>e</sup>, H.Y. Chao<sup>j</sup>, C.N. Chiou<sup>j</sup>, S. Cihangir<sup>a</sup>, R.P. Ely<sup>e</sup>, E. Engels Jr.<sup>g</sup>, A. Franceschi<sup>c</sup>, A. Barbaro-Galtieri<sup>e</sup>, M. Guerra<sup>a</sup>, A.F. Garfinkel<sup>h</sup>, G. Gillespie<sup>a</sup>, D. Glenzinski<sup>d</sup>, H. Gonzalez<sup>a</sup>, S. Gonzalez<sup>a</sup>, C. Grimm<sup>a</sup>, C. Haber<sup>e</sup>, T. Hawke<sup>a</sup>, M. Hrycyk<sup>a</sup>, J. Incandela<sup>a</sup>, E. Kajfasz<sup>a</sup>, R. Klein<sup>a</sup>, S. Kleinfelder<sup>e</sup>, M. Kruse<sup>h</sup>, B. Lundberg<sup>a</sup>, F. Mando<sup>b</sup>, J. Matthews<sup>f</sup>, A. Menzione<sup>c</sup>, C. Nelson<sup>a</sup>, A. Paccagnella<sup>b</sup>, M. Paulini<sup>e</sup>, M.D. Peters<sup>e</sup>, N. Praticelli<sup>b</sup>, F. Raffaelli<sup>c</sup>, P. Ratzmann<sup>a</sup>, A. Schindler<sup>e</sup>, F.G. Sciacca<sup>c,\*</sup>, L. Scott<sup>a</sup>, M.D. Shapiro<sup>e</sup>, N.M. Shaw<sup>h</sup>, T. Shaw<sup>a</sup>, P. Shepard<sup>g</sup>, P. Singh<sup>g</sup>, J.E. Skarha<sup>d</sup>, F.D. Snider<sup>d</sup>, L. Song<sup>a</sup>, J. Spalding<sup>a</sup>, D. Stuart<sup>a</sup>, P. Tipton<sup>i</sup>, S. Tkaczyk<sup>a</sup>, K. Tollefson<sup>i</sup>, D. Tousignant<sup>a</sup>, K. Turner<sup>a</sup>, C.H. Wang<sup>j</sup>, M.J. Wang<sup>j</sup>, G. Watts<sup>i</sup>, H. Wenzel<sup>e</sup>, S.C. Wu<sup>j</sup>, W. Yao<sup>e</sup>, R. Yarema<sup>a</sup>, J.C. Yun<sup>a</sup>, F. Zetti<sup>c</sup>

<sup>a</sup> Fermi National Accelerator Laboratory, Batavia, Illinois 60510, USA

<sup>b</sup> INFN Padova, Padova, Italy

<sup>c</sup> INFN Pisa, Pisa, Italy

<sup>d</sup> Johns Hopkins University, Baltimore, Maryland 21218, USA

<sup>e</sup> Lawrence Berkeley Laboratory, Berkeley, California 94720, USA

<sup>f</sup> University of New Mexico, Albuquerque, New Mexico 87131, USA

<sup>g</sup> University of Pittsburgh, Pittsburgh, Pennsylvania 15104, USA

<sup>h</sup> Purdue University, West Lafayette, Indiana 47907, USA

<sup>i</sup> University of Rochester, Rochester, New York 14627, USA

<sup>j</sup> Academia Sinica, Taiwan, ROC

### Abstract

The Collider Detector at Fermilab (CDF) radiation hardened silicon vertex detector (SVX') is described. The new detector has several improvements over its predecessor such as better signal to noise and higher efficiency. It is expected to have a radiation tolerance in excess of 1 Mrad. It has been taking data for several months and some preliminary results are shown.

### 1. Introduction

For Tevatron Collider run 1B a new silicon vertex detector (SVX') has been installed in the CDF detector to replace the SVX [1–3], the first silicon vertex detector to be successfully operated in a hadron collider environment. The new detector has the same overall configuration as the SVX; however, several differences lead to significant improvements over its ancestor. It is equipped with a radiation hard readout chip with higher gain [SVX IC, Rev H (SVXH3)] and it is AC coupled, so that radiation induced leakage currents will not saturate the input of preamps; it

has lower noise (due mostly to the AC coupling) and complete  $\phi$  coverage for the inner layer.

### 2. Description of the SVX'

A complete description of the SVX detector can be found in Refs. [1,2]. The overall detector configuration remains unaltered for SVX'. We will emphasize the differences between the two detectors.

#### 2.1. Geometry

SVX' modules (also referred to as barrels) consist of four layers of silicon strip detectors segmented into twelve 30° wedges. Two such barrels are aligned along the beam

\* Corresponding author.

direction with a gap between them of 2.15 cm at  $z = 0$ . The basic detector element is called a ladder and there are 96 such elements in the complete detector. The geometry of the inner layer has been significantly changed in order to achieve complete  $\phi$  coverage. The ladders of the inner layer are overlapped at the edges. A  $0.17^\circ$  overlap is obtained for the SVX' corresponding to 0.24 strips whereas SVX has a  $1.26^\circ$  gap. The inner layer is also closer to the beam line by  $\sim 1.5$  mm at a radius of 2.86 cm.

## 2.2. Front end readout chip

The front end readout circuit is the SVX chip Revision H (was revision D [4,5] for SVX). It was fabricated in 1.2  $\mu\text{m}$  CMOS technology and the CMOS process was radiation hard. The chip is expected to tolerate more than 1 Mrad of radiation. Typical gains are around 21 mV/fC at the input capacitance typical of our detectors, which is  $\approx 30$  pF for a full strip length of 25.5 cm.

Table 1  
Comparison of SVX and SVX'

Feature	SVX	SVX'
Channels		46080
z coverage		51.1 cm
Gap at $z = 0$		2.15 cm
Radius L0	3.0049 cm	2.8612 cm
Radius L1		4.2560 cm
Radius L2		5.6872 cm
Radius L3		7.8658 cm
Overlap L0	$-1.26^\circ$ (gap)	$0.17^\circ$ (.24 strip)
Overlap L1		$0.32^\circ$ (4 strip)
Overlap L2		$0.30^\circ$ (4 strip)
Overlap L3		$0.04^\circ$ (0 strip)
Silicon	DC	one-sided AC FOXFET bias
Passivation	none	silox
Atmosphere	Ar/ethane + alcohol	dry nitrogen
Readout chip	SVX IC Rev.D	SVX IC Rev.H3
Sampling	quadruple	double
Noise	2200 electrons	1300 electrons
Gain	15 mV/fC	21 mV/fC
Res/ integrate		$3.5 \mu\text{s}$
Readout time	$2.7 \mu\text{s}$	$2.1 \mu\text{s}$
Rad limit	$> 20$ krad	$> 1$ Mrad
Bad channels	1.59%	1.73%
Occup. typ	7–10%	5%
Occup. max	12–20%	25%

## 2.3. Pedestal, noise, bad channels

The silicon detectors used in the ladder construction are single-sided FOXFET biased and AC coupled [6]. The SVX was DC coupled and in order to subtract the effect of varying strip to strip leakage currents it had to be operated in quadruple sample & hold mode with two successive charge integrations. With the AC coupled detectors we operate the SVX chip in double sample & hold mode with only one charge integration to determine the outgoing signal so the noise is lower by a factor  $\sqrt{2}$  compared to the SVX. Data taken without incident particles were analyzed to get the average pulse height (the pedestal) and standard deviation (the noise) of every channel. Typical values of the noise are around 1300 electrons (10.8 ADC counts) to be compared with a value of roughly 2200 electrons for SVX. Channels showing large deviations from the expected behavior (mostly higher noise) and channels not bonded to the chip because of the coupling capacitance being damaged or shorted are  $\approx 1.7\%$  of the total to be compared with  $\approx 1.6\%$  for SVX at the beginning of its operation. Another important improvement due to the AC coupling is the ability to operate the detector without saturating the SVXH3 readout chip preamp even when radiation damage to the silicon leads to a significant increase in leakage current for silicon strips. During its operation the SVX' is expected to receive a radiation dose of 60 krad. Measurements done on the SVX detector show a leakage current increase rate of 2.7 nA/krad per strip for the inner layer. The SVXH3 preamp will saturate at 80 nA input current. Table 1 is a comparative summary of the features of SVX' and SVX.

## 3. Collider data analysis

Results reported in the following sections refer to the operation of the detector in CDF for the Tevatron Collider run 1B. Full event reconstruction using the CDF offline was performed on samples of data from run 1B. Signal-to-noise ratio, hit efficiency, track quality, hit and impact parameter resolution measurements are preliminary.

### 3.1. Charge collection

Clusters are defined as contiguous groups of strips whose pulse height,  $q$ , is greater than  $M$  times their noise,  $\sigma$ . We have chosen  $M = 4.0, 2.5, 2.0$  for one strip, two strip and larger clusters respectively. These were the same operational values used for SVX. Studies carried out on cosmic ray and collision data to reoptimize  $M$  for better hit efficiency and noise rejection resulted in maintaining the previous values. The cluster position is defined as the charge centroid:  $x = \sum x_i q_i / \sum q_i$ . To select a clean sample of clusters, we require that they: a) belong to a four hit track reconstructed by the CDF tracking code, b) do not

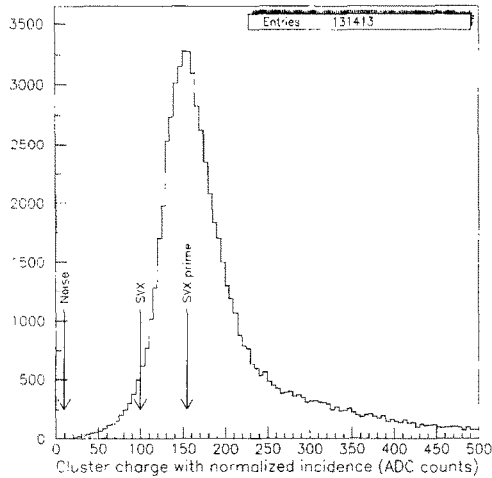


Fig. 1. Pulse height distribution (ADC).

contain any bad channels. The resulting distribution (Fig. 1) shows the most probable charge to be 155 ADC and a width of 23 ADC. Using the measured value of noise reported in Section 2.3 we can quote a signal-to-noise ratio of about 15. Also shown in Fig. 1 are the noise and signal values as measured in SVX.

### 3.2. Hit efficiency

To determine the hit efficiency of a target layer, we select a sample of tracks having hits on three layers and look for a fourth hit in a window of  $\pm 10$  strips around the track intersection with the fourth layer. The efficiencies calculated in this way are 92.01% for the inner layer, 95.0% for the outer layer, 96.8% and 96.9% for the two internal layers. For all layers these numbers include inefficiencies due to the presence of microbonding regions (1.7% of the silicon region) between the three silicon crystals that make up a ladder as well as effects due to unusable channels (1.7% of the total number of channels) and effective detector inefficiency. The results for the inner and outer layers are additionally affected by the geometric acceptance at  $z = 0$  and at the edges of the detector. Comparing the expected inefficiency for the two internal layers due to microbonding regions and to unusable channels with the numbers quoted above, we find that the effective detector inefficiency is negligible (less than 1%).

### 3.3. Occupancy

The detector is operated in sparse mode to read out only channels whose signal is above a hardware threshold so that the readout time and data size are set by hit occupancy rather than total channel count. The value of the thresholds is optimized in order to provide minimum occupancy and 100% efficiency for half a MIP. The typical

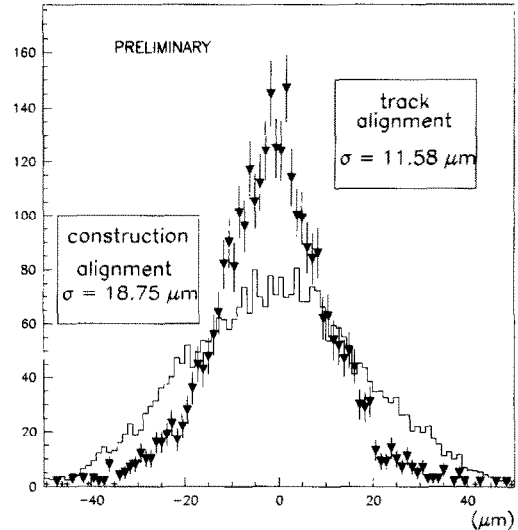


Fig. 2. Residuals for 2 and 3 strip clusters combined.

occupancy observed at these thresholds is 5%. Peak values (25%) are observed on one of the 12 angular sectors of the detector. This is due to a reoptimization of the thresholds for that sector to account for one ladder showing large deviations from the typical behaviour. Typical values for occupancy in SVX were between 7% and 10%. The SVX chip is operated with a readout cycle of 2.1  $\mu\text{s}/\text{channel}$  for SVX' (was 2.7 for SVX).

### 3.4. Position resolution and alignment

The position resolution of a target layer is evaluated using a sample of tracks having hits on the other layers.

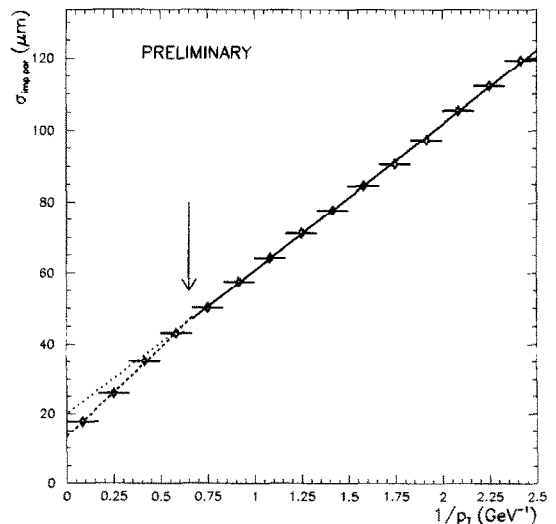


Fig. 3. Impact parameter resolution ( $\sigma_{\text{res}}$  vs  $1/P_t$ ).

Tracks are fitted using only these hits. We then plot the distribution of the distance of track intersections from reconstructed cluster centroids on a target layer (Fig. 2). The mean of this residual distribution is used to evaluate the ladder alignment constants, while its width,  $\sigma_{\text{res}}$ , is related to the position resolution,  $\sigma_{\text{pos}}$ , by the equation:  $\sigma_{\text{res}}^2 = \sigma_{\text{pos}}^2 + \sigma_{\text{fit}}^2$ , where  $\sigma_{\text{fit}}$  is the contribution of the errors on fitted track parameters. For one, two and three strip clusters we find  $\sigma_{\text{pos}} = 13, 11, 16 \mu\text{m}$ . The alignment constants are used iteratively to correct for misalignments in  $z$ ,  $\phi$  and radial direction, with respect to the nominal detector position. This alignment procedure has already produced significant improvements of track quality and resolution (Fig. 2). When the procedure is complete we expect a further improvement of the resolution values. A preliminary evaluation of the impact parameter resolution gives an asymptotic value  $\sigma_{\text{impar}} = 13 \mu\text{m}$ . In Fig. 3 one can distinguish the contribution to the impact parameter resolution from multiple scattering at low  $P_t$  and from the intrinsic detector resolution at high  $P_t$ .

#### 4. Conclusions

The new CDF silicon vertex detector is being operated at Fermilab for the Collider run 1B. Performance of the detector has been evaluated during several months of data taking. We measured a signal-to-noise of 15, an efficiency  $> 99\%$ , an average position resolution of  $11.6 \mu\text{m}$ , and an asymptotic impact parameter resolution of  $13 \mu\text{m}$ .

#### References

- [1] D. Amidei et al., Nucl. Instr. and Meth. A 289 (1990) 388.
- [2] D. Amidei et al., FERMILAB-PUB-94/024-E, submitted to Nucl. Instr. and Meth.
- [3] D. Amidei et al., CDF2061 (1993).
- [4] S.A. Kleinfelder, IEEE Trans. Nucl. Sci. NS-35 (1988) 171.
- [5] C. Haber et al., IEEE Trans. Nucl. Sci. NS-37 (1990) 1120.
- [6] Manufactured by Micron Semiconductor Ltd., 1 Royal Buildings, Marlborough Road, Churchill Ind. Estate, Lancing, Sussex BN15 8UN, England.